HHS Public Access

Author manuscript

Ann Biomed Eng. Author manuscript; available in PMC 2018 April 01.

Published in final edited form as:

Ann Biomed Eng. 2017 April ; 45(4): 990–1002. doi:10.1007/s10439-016-1735-y.

Development of a smart pump for monitoring and controlling intraocular pressure

Simon A. Bello[1], **Sharad Malavade**[2], and **Christopher L. Passaglia**[1,2]

[1]Department of Chemical & Biomedical Engineering, University of South Florida, Tampa, FL 33620

[2]Department of Ophthalmology, University of South Florida, Tampa, FL 33620

Abstract

Animal models of ocular hypertension are important for glaucoma research but come with experimental costs. Available methods of intraocular pressure (IOP) elevation are not always successful, the amplitude and time course of IOP changes are unpredictable and irreversible, and IOP measurement by tonometry is laborious. Here we present a novel system for monitoring and controlling IOP without these limitations. It consists of a cannula implanted in the anterior chamber of the eye, a pressure sensor that continually measures IOP, and a bidirectional pump driven by control circuitry that can infuse or withdraw fluid to hold IOP at user-desired levels. A portable version was developed for tethered use on rats. We show that rat eyes can be cannulated for months without causing significant anatomical or physiological damage although the animal and its eyes freely move. We show that the system measures IOP with <0.7mmHg resolution and <0.3mmHg/month drift and can maintain IOP within a user-specified window of desired levels for any duration necessary. We conclude that the system is ready for cage- or bench-side applications. The results lay the foundation for an implantable version that would give glaucoma researchers unprecedented knowledge and control of IOP in rats and potentially larger animals.

Keywords

glaucoma; rat; telemetry; eye; implant; closed loop control

INTRODUCTION

Elevated intraocular pressure (IOP) has been identified as a major risk factor for glaucoma[14,31], an eye disease that causes gradual loss of vision and eventually blindness if left untreated. To better understand the etiology and pathophysiology of the disease, several experimental models have been developed in mice, rats, rabbits, pigs, and monkeys. The models raise IOP by increasing the resistance of aqueous outflow pathways of the eye through a variety of techniques, including laser photocoagulation of trabecular meshwork[10,34], hypertonic saline injection into limbal vessels[7,23], cauterization of episcleral veins[27,30], and ghost red blood cell[25] or microbead[29,36] injection into the anterior chamber.

Corresponding author: Dr. Christopher L. Passaglia, Department of Chemical and Biomedical Engineering, University of South Florida, 4202 E Fowler Ave, Tampa, FL 33620. Phone: 813-974-7140, passaglia@usf.edu.

The reduced aqueous outflow leads to chronic ocular hypertension and progressive injury of the retina and optic nerve like that seen in human glaucoma.

While experimental models provide much insight, available methods of glaucoma induction and pressure monitoring have important limitations. Firstly, the failure rate is high so many animals do not experience a significant IOP increase. Secondly, some methods need repeating to achieve chronic IOP elevation and induction success might not be apparent for weeks after treatment[7,23,36], while other methods produce a rapid IOP change that returns to baseline levels over time[30,34]. Thirdly, the researcher has no control over the amplitude or time course of IOP elevation. The detailed pressure history to which treated eyes are exposed can range widely across animals, making it more difficult to correlate IOP exposure with glaucoma onset and progression. Fourthly, damage done to aqueous outflow pathways cannot be experimentally reversed so the capacity of the eye to recover from glaucomatous injury cannot be investigated. And fifthly, IOP is usually measured by hand with a tonometer. Tonometers can provide only an indirect and sporadic record of the pressure history of an eye, which is less accurate and more variable in smaller eyes having high corneal curvature[1]. The sparse pressure data hamper examination of relationships between glaucoma and IOP dynamics[4,5,16], which have been shown to fluctuate on multiple time scales due to blood pulsation, respiration, and endogenous biological rhythms[2,8,15,17,19].

This manuscript describes a novel IOP control system that can overcome limitations of existing glaucoma models. We refer to the system as iPump because it consists of an autonomous bidirectional pressure-sensing pump connected to a cannula implanted in the eye. Data are provided on: i) the resolution, noise level, and long-term stability of pressure measurements *in vitro*, ii) the anatomical and physiological status of rat eyes implanted with a cannula for months, and iii) the ability of the system to maintain IOP of anesthetized rats at any level desired by the user. The results demonstrate that a portable iPump system is ready for tethered use on rats and for miniaturization into an implantable device. The technology promises, for the first time, to provide researchers complete knowledge and control of IOP in conscious behaving animals.

MATERIALS AND METHODS

Animal preparation

Experiments were performed on adult Brown-Norway rats (300-400g) housed under a 12hr-12hr light-dark cycle and fed a standard daily diet. All procedures were approved by the Institutional Animal Care and Use Committee of the University of South Florida in accordance with NIH guidelines.

System instrumentation

The iPump system includes a cannula, two pressure sensors, control circuitry, and a bidirectional fluid pump (figure 1(A)). The cannula is implanted in the anterior chamber of the eye and conducts IOP to one pressure sensor while a second identical sensor measures atmospheric pressure. The controller circuit compares sensor outputs with a target IOP level specified by the user and commands the pump to withdraw or inject fluid through the

cannula so as to set and hold IOP at the user-specified level. A 7-ml reservoir is connected to the pump that can be drained or refilled as needed.

A portable system was constructed for research use (figure (1B)). The cannula is a fine polyimide tube (ID: 100 μm, OD: 130 μm, MicroLumen, Oldsmar, FL) filled with sterile artificial aqueous humor[20] (130 mM NaCl, 5 mM KCl, 5 mM $NaHCO_3$, 1 mM $CaCl_2$, 0.5 mM $MgCl_2$, 5 mM glucose, 20 mM HEPES, pH 7.25). The cannula runs subdermally to a custom head mount (10 mm) that connects to the iPump via 30G Teflon tubing (length: 35cm, Zeus, Branchburg, NJ) and prevents animals movements from retracting the cannula tip from the eye. The system interfaces with a computer via a USB connection, which provides power and data lines. A custom Labview program sends the desired IOP set point to the device and records IOP and pump command signals at 1 Hz. The iPump can operate in two modes. In open-loop mode, only the pressure sensors (TBPDANS005PGUCV, Honeywell, Morristown, NJ) are powered and IOP is reported. In closed-loop mode, the control circuitry and pump (MP6, Servoflo, Lexington, MA) are also powered and IOP is clamped within a user-specified window of the set point. A ±2 mmHg window was used here. IOP control is achieved by varying the pump rate or pump duty cycle. In the latter case, pump rate was fixed at 2 μL/min.

Calibration and bench testing

The iPump system was calibrated by connecting the cannula (length: 10 mm) to a saline reservoir and mercury manometer via a three-way stopcock. Reservoir height was varied, and the offset voltage and gain of the pressure transducer were mapped to mmHg. Long-term stability was evaluated by fixing reservoir height and recording pressure continually for 90 days. The reservoir was covered to prevent evaporation, and fluid level was regularly checked to verify that hydrostatic pressure stayed constant. Room temperature was concurrently monitored with a thermistor. Drift in transducer output was approximately linear and quantified by regression. System compliance was determined by sealing the cannula tip, injecting known fluid volumes into the line, and estimating the slope of measured pressure changes by linear regression. System accuracy was evaluated by recording IOP in dead rats with an independent commercial pressure transducer (5110, Stoelting, Wood Dale, IL). Animals were anesthetized with a mixture of ketamine and xylazine (50 and 7 mg/kg, IP), and an eye was cannulated with two 33G needles mounted on micromanipulators. One needle was connected to the iPump cannula (length: 10 mm) and the other to the commercial transducer. Animals were then euthanized with Euthasol (>50 mg/kg, IP), and sensor outputs were digitized to computer. After IOP fell to 0 mmHg the system was run at pump rates of 1-4 μL/min for several minutes each, and sensor differences in IOP onset and amplitude were quantified. System dynamics were separately evaluated by measuring the time needed for each rate setting to raise IOP by 20 mmHg and the time needed for IOP to decay back to 0 mmHg afterwards.

Cannula implantation

The feasibility of long-term implantation of a cannula in the anterior chamber was examined in 20 rats. Key to success was the fabrication of a custom mold that shaped the tip to the curvature of rat eyes and angled it into the iridocornealspace. The mold was created by

bending a 23G needle into a three-dimensional figure Z. The cannula was threaded through the curved needle and permanently re-shaped by apply heat to the needle with a cautery pen (figure (2A)). Animals were anesthetized on the day of implantation with the ketamine-xylazine mixture, supplemented as needed. The head was secured in a stereotaxic, eyes were instilled with mydriatic (1% cyclopentolate hydrochloride), and one eyelid was retracted. A 2-mm incision was made in the conjunctiva parallel to the limbus near the nasal canthus, and conjunctival tissue was dissected anteriorly to make space for cannula attachment to the sclera (figure (2B)). The cannula was filled with artificial aqueous humor and fed into a 23G needle, which was slid through the incision to the medial orbital wall and redirected vertically to exit the scalp. The needle was removed, the cannula was cut (length: 20 mm), buried under the skin, and the Z-shaped end was anchored with 2 to 3 half-thickness scleral sutures. A hole was tunneled into the anterior chamber with a 33G needle that was directed under the circumlimbal venous plexus and angled to avoid iris contact. The cannula tip was passed through the hole until a short length (~1 mm) was visible in the eye (figure (2C)). The tip was anchored with 2 additional half-thickness scleral sutures, the conjunctiva was closed with sutures, and the eyelid was released. Throughout the procedure corneas were kept moist with ophthalmic solution. Every 12 hours for 3 days after surgery animals were given carprofen (5 mg/kg, IM) for pain relief, and each eye was instilled with 1% cyclopentolate to prevent iris attachment and 1% prednisone to combat inflammatory processes. The cannula was implanted in the right eye, the left eye served as a control. The non-implanted end was not connected to the iPump system in these animals as the experimental objective was to develop an implantation procedure that can last for weeks without permanently deflating or damaging the eye. In initial experiments, Seidel tests were conducted during the first post-operative month to check for aqueous leakage. The tests were done by touching a fluorescein strip to the cornea and observing dye clearance at the implant site with an ophthalmoscope.

Tonometer measurements

IOP was measured once per week in both eyes of implanted rats with a handheld tonometer (Tono-Pen XL, Medtronic, Sarasota, FL). Measurements were taken around noontime to control for circadian fluctuations in IOP level[22]. Animals were anesthetized with 2% isoflurane and rested on a thermal pad. A total of 6 readings were taken from each eye and averaged.

Electroretinogram recordings

Electroretinograms (ERGs) were periodically recorded from implanted rats to assess the physiological health of the retina. Recordings were made while the animals were anesthetized for tonometer measurement. A ring-shaped gold electrode was placed on the cornea of each eye, and platinum needle electrodes were inserted in the scalp and tail to respectively serve as reference and ground. Animals were dark adapted for ~1 hour and then a series of 30 brief (10 ms) flashes were delivered simultaneously to both eyes with an inter-flash interval of 3 s and intensity of 0.5, 1, or 2 kcd/m^2. Flashes were emitted by a LED (Vishay TLCTG5800, Newark Electronics, Palatine, IL) positioned 1 cm in front of each cornea. Recorded signals were differentially amplified (2000x) and filtered (0.1-1000 Hz) by

a multichannel bioamplifier (Xcell-3x4, FHC Inc., Bowdoin, ME) and digitized at 1000 Hz to computer via a custom LabView program.

Ocular imaging

The iridocorneal angle and fundus of implanted rats were inspected every month to assess implant stability, ocular fluid clarity, and ocular tissue health. Inspections were made while animals were anesthetized for tonometer measurement. The iridocorneal angle was imaged using a stereomicroscope fitted with a digital camera and bright light source (Motic SMZ-168, Ted Pella Inc, Redding, CA). The fundus was imaged in the same manner by flattening the cornea with a glass coverslip. In two cases, implanted animals were anesthetized with the ketamine-xylazine mixture and their head was mounted in an OCT scanner (Spectralis II, Heidelberg Engineering, Franklin, MA). The anterior and posterior half of the eye was scanned along several planes to visualize cannula placement and retinal vasculature in greater detail. Afterwards, animals were euthanized and both eyes were enucleated for histological processing.

Histological processing

The eyes of 5 implanted rats were processed histologically to assess ocular tissue damage. Both eyes were quickly enucleated from euthanized animals, washed in PBS, immersed in 4% paraformaldehyde, and stored at 35° F. One week later the eyes were processed for paraffin embedding using standard protocols, and the paraffin block was cut with a microtome (RM2235, Leica Microsystems Inc, Buffalo, NY) in 6-μm sections parallel to the implanted cannula. Tissue sections were mounted on glass slides and stained with hematoxylin and eosin (HE). Select sections were stained with Giemsa solution to check for inflammatory products.

System testing in anesthetized animals

The *in vivo* performance of the complete iPump system was assessed in 5 rats. After implanting a cannula (length: 20 mm) for >3 days to allow for wound closure, animals were anesthetized with the ketamine-xylazine mixture. A catheter was inserted in the femoral vein, and anesthesia was maintained for remainder of the experiment via intravenous infusion of ketamine (30 mg/kg/hr), dextrose (600 mg/kg/hr), and physiological saline. The head was mounted in a stereotaxic, and the body was rested on a heating blanket under temperature control via a rectal thermometer. Needle electrodes were inserted to record the ECG. Eyes were instilled with mydriatic and fitted with clear contact lenses to prevent corneal drying. The scalp was opened to expose the implanted cannula, which was then connected to a fluid-filled 30G needle tethered by PTFE tubing and a three-way stopcock to the iPump system. The third port was closed except to extract bubbles in the line or null the system to atmospheric pressure. Data were collected while vitals (heart rate, ECG waveform, body temperature) remained at healthy levels. The system was run in open-loop mode for two animals and closed-loop mode for three animals. Before activating feedback control the implanted eye was undisturbed for 15 minutes to determine baseline IOP. Afterwards, the system was programmed to step IOP to levels ranging from 5-35 mmHg and hold IOP within ±2 mmHg of the target level for 2-4 hours.

Data analysis

Statistical significance was assessed by a two-sample *t*-test with an alpha level of 0.05 using SigmaPlot software (San Jose, CA). Results are expressed in terms of mean ± standard deviation.

RESULTS

Specification of system properties

The iPump system was calibrated by connecting the cannula to a variable-height fluid reservoir and mercury manometer. Figure 3(A) plots the recorded pressure as hydrostatic pressure was raised from 0 to 100 mmHg and then released. The system responds instantly to step changes in pressure with a step-like waveform. Figure 3(B) plots the average pressure reading for each pressure step. Sensor output is linear over the range tested, which more than spans normal and glaucomatous IOP levels. Sensor output is also very accurate. The standard deviation of noise in the records is <0.5 mmHg for all applied pressures. Long-term stability was evaluated by applying constant hydrostatic pressure to the iPump system for several weeks via the water column (n = 3). Figure 3(C) shows the signal recorded by a system that was continually exposed to 40 mmHg. Linear regression of the data yielded an average pressure reading of 40.4 ± 0.4 mmHg. The regression slope was −0.05 mmHg/week for the illustrated device and +0.04 and −0.02 mmHg/week for two others tested, amounting to a total drift of <1 mmHg over 3 months. Figure 3(C) shows that system output was insensitive to room temperature fluctuations from 22 to 26°C ($R^2 = 0.003$). Temperatures outside the normal operational range were not examined. These results indicate that the iPump system can accurately record pressure for months on end.

IOP measurement accuracy was evaluated by cannulating the anterior chamber of rat eyes with two needles and connecting one to the iPump system and the other to a calibrated commercial pressure sensor. The animal was then euthanized to eliminate biological disturbances. Figure 3(D) shows the IOP recorded *in situ* by the two sensors as the iPump perfused the eye at different rates. It can be seen that the system closely tracked IOP measurements by the commercial sensor. Figure 3(E) shows the average discrepancy in sensor output across animals (n = 4). The discrepancy was virtually zero at rest or when the pump was off (0.2 ± 0.2 mmHg) and increased with pump rate, with the system overestimating IOP by 1.4 ± 0.4 mmHg at 4 μL/min ($p < 0.05$). The rate dependence reflects the hydraulic impedance of the cannula and tether tubing, which causes a hydrodynamic pressure drop between the eye and iPump sensor. According to Poiseuille's law the resistance (R) of each tube is given by $R = 8\eta L/\pi r^4$, where L is tube length, r is lumen radius, and η is fluid viscosity (8.75×10^{-8} mmHg·min at body temperature[9]). The predicted system resistance is thereby 0.36 mmHg·min/μl, which is consistent with the data (dashed line). Figure 3(F) shows that IOP dynamics scale nonlinearly with pump rate. It took the system nearly 30 min to raise IOP by 20 mmHg at 1 μL/min and just 5 min at 2 μL/min. The exact dynamics depend on aqueous volume, outflow facility, ocular compliance, and system tubing compliance. The latter was 0.12 ± 0.01 μL/mmHg (n = 3, data not shown). A tradeoff thus exists between accuracy of IOP measurement and speed of IOP alteration, so the pump

rate of the iPump system was fixed at 2 μL/min to achieve maximum speed with minimal loss of accuracy.

Visual evaluation of implanted eyes

In conjunction with system development, the feasibility of implanting a cannula in rat eyes was explored. Initially, the cannula was run straight from the scalp into the anterior chamber, but this approach usually failed during the first post-surgical week because of cannula migration into or out of the eye. An implantation procedure was thereby devised in which the cannula was pre-shaped to run from the scalp to the nasal canthus and 30-45° around the limbus before entering the eye (figure (2)). Cannulas were implanted in 20 rat eyes using this procedure with a success rate of 80%. An implant was deemed a success if it remained in place for >2 weeks without causing intraocular inflammation, infection, or injury. Figure 4(A) shows pictures of two rat eyes that were implanted for several months. It can be seen that the aqueous humor is clear, the cornea and iris are undamaged, and the cannula position is unchanged although the eye could freely blink and rotate. Figure 4(B) shows these and other implanted eyes at higher magnification. The wound is healed over the cannula, and the tip shows little-to-no fibrosis. The cornea of some animals exhibited slight opacification and blood vessel growth from contact with the tip (asterisk) while the rest of the eye looked normal. No leakage of aqueous humor was detected at the implant site based on Seidel's tests performed during the first post-operative month (n = 3, data not shown).

Implant placement within the anterior chamber was inspected in closer detail. Figure 5(A) shows a cross-section of the iridocorneal angle of the eye implanted for 3 months in Figure 4(A). The cannula can be seen to pass under limbal vessels through the sclera and into the anterior chamber through the trabeculum. The path of entry was the same for all eyes examined (n = 4) except the track sometimes intersected the iris root. A fine outgrowth of tissue can also be seen between the corneal endothelium and cannula (arrowhead). Figure 5(B) shows OCT images of the iridocorneal angle of the same eye in the live animal. The angle is viewed along longitudinal and transverse planes of the implant. The tip rested against the inner wall of the cornea, away from the iris and lens where it could get clogged or cause serious damage. Corneal curvature was largely undistorted as tip pre-shaping helped to blunt contact stresses that could cause corneal ulceration. The fundus of implanted eyes was periodically inspected for signs of damage by direct ophthalmoscopy (n = 20) and at experiment end by OCT imaging (n = 2). Figure 5(C,D) shows fundus images for the implanted eye above. It can be seen that vitreous humor is clear and retinal vasculature and optic nerve striation patterns exhibit no abnormalities.

Implanted eyes were processed histologically for signs of tissue inflammation and damage (n = 4). Figure 6(A) shows a HE stained section of the iridocorneal angle of the implanted rat eye above. The parallel layering of corneal stroma fibrils was undisturbed except by the limbus where some tortuosity and inflammatory reaction is present at the insertion site. A thin outgrowth of scar tissue can also be seen between the cannula and corneal endothelium, which extended toward the tip (figure 5(A)). The outgrowth was inconspicuous under direct ophthalmoscopy (figure 4). The lumen and inner wall of the cannula was devoid of cellular matter. Figure 6(B) shows a HE stained section of retinal tissue from the same animal. No

abnormality was noted in retinal layer thickness or cell density. By all visual indications, implanted rat eyes are healthy and have accepted the cannula for life.

Physiological evaluation of implanted eyes

The IOP of implanted eyes was regularly monitored with a tonometer. Figure 7(A,B) shows bilateral IOP records from two rats. Readings from the implanted eye were stable over several weeks and deviated any given day by <3 mmHg from the non-implanted eye. As a result, mean IOP was not significantly different between the eyes of these and all other animals examined (n = 8, $IOP_{implant}$ = 19.5 ± 3.3 mmHg, $IOP_{control}$ = 20.0 ± 3.2 mmHg). The data demonstrate that cannula implantation did not cause chronic aqueous leakage or a foreign body response that alters aqueous humor production or outflow facility.

Retinal health of implanted eyes was assessed with ERG recordings. Figure 7(C,D) shows full-field ERG signals recorded from two anesthetized rats for flashes of one or more intensity presented under dark-adapted conditions. Both the implanted and non-implanted eyes generated a- and b-waves of similar amplitude and time course. ERG records were collected 1-2 months after implantation from a group of rats (n = 4), and the relative a- and b-wave amplitudes and implicit times of both eyes were compared. No significant difference in any of these parameters was noted (difference in a-wave amplitude: 1 ± 7 μV, p=0.767, b-wave amplitude: 5 ± 11 μV, p=0.539, a-wave implicit time: 0.7 ± 2.4 ms, p=0.779, b-wave implicit time: 3.1 ± 6.2 ms, p=0.595). The data lend further support that the retina was not injured directly by the implantation procedure or indirectly by tissue responses to the ocular implant.

System performance in anesthetized animals

Once device electronics were tested and cannulation procedure was developed, the performance of the complete system was evaluated *in vivo* from anesthetized rats in a sound- and light-proof room. Figure 8(A) shows the IOP record of an implanted eye over a 28-hour period recorded with the iPump in open-loop mode. After cannula insertion at noon, IOP settled at a daytime level of ~16 mmHg as resting aqueous outflow and fluid volumes were restored. IOP later increased to ~22 mmHg after daytime lighting would normally have turned off at 6PM, and it remained at this level until the following morning when IOP decreased to ~14 mmHg after daytime lighting would normally have turned on at 6AM. The nighttime elevation is consistent with prior observations of circadian IOP rhythms in rodents[15,22]. It can be seen that IOP also fluctuated at faster time scales, especially at night in this recording, although the animal was anesthetized for the entire experiment. Figure 8(B) shows that the fluctuations are irregular and ranged 2-4 mmHg in amplitude in this rat. The *in vivo* variability averaged 2.1 ± 1.5 mmHg across all IOP recordings (n = 5). This is significantly greater than the *ex vivo* variability (figure 3), which implies that the IOP noise is produced by the animal. Figure 8(C) shows the IOP record of an implanted eye in which the iPump was programmed to hold pressure for 2 hours at 25, 45, and 35 mmHg. Upon activation of closed-loop control (asterisk), IOP increased from its resting level of ~15 mmHg to ~25 mmHg as the system injected fluid into the eye. Figure 8(D) shows that, once target IOP was reached, the system ceased pumping and IOP slowly decreased as the eye cleared the excess fluid. When IOP fell 2 mmHg below the target level, the system resumed

pumping and returned IOP to ~25 mmHg. The cycle repeated until the target level was switched, at which time the system adjusted the pump duty cycle and IOP was maintained at ~45 and ~35 mmHg. Figure 8(E) summarizes the distribution of measured IOP values across animals for an iPump control window of ±2 mmHg. The distribution was comparable to the window size for all target IOP levels. For example, IOP was kept between 22.4 to 27.8 mmHg over a 2-hr period when the system set point was 25 mmHg.

DISCUSSION

This study introduces a portable telemetric system that can continuously monitor and autonomously control IOP in rats, and potentially larger animals. The iPump system was extensively tested and its performance specifications were quantified. We show that: i) a cannula can be placed in the anterior chamber of rat eyes for months without slipping out, damaging iridocorneal tissues, or altering ocular physiology, ii) the system can accurately read pressure for months without drift while compensating for ambient fluctuations in barometric pressure and room temperature, and iii) the system can measure and hold IOP of rat eyes within a programmable window of any set point desired by the user.

The study also introduces a surgical procedure for long-term cannulation of the eye. A key step was pre-shaping the cannula tip to eye curvature so that it minimally presses against internal structures and bends at strategic suture points that prevent cannula retraction. Implant longevity appears limited only by the research objective and animal age, as few implants have failed since the procedure was developed. The cannula tip remained visibly open months after implantation. Fibrous tissue could though be seen growing along the cannula at higher magnification and reached the tip in some animals. The tissue growth depends on tip placement within the anterior chamber[19]. It presents a potential complication for long-term measurements of IOP that we are working to solve since tip clogging would cause transducer readings to deteriorate. It is less a concern for experiments that use the system for closed-loop IOP control because fluid would be continually moving through the tip.

Broader applications of the technology

The iPump system was conceived as a tool for reliably inducing ocular hypertension or for restoring hypertensive eyes to normal IOP levels. Recent work has indicated that glaucoma onset and progression may depend not just on IOP but more specifically on the pressure gradient across the lamina cribrosa[6,24,26], a weblike collageneous structure through which optic nerve fibers exit the eye. The translaminar gradient is a function of IOP and intracranial pressure (ICP), raising interest in a possible role of ICP dynamics in the disease. By implanting the cannula in cerebral ventricles, the iPump system can also be used to monitor and control ICP. It could even be used to set the translaminar gradient. Since the system has two pressure sensors, it could simultaneously measure IOP and ICP while controlling one of them so as to hold the gradient at a user-specified amount.

Abnormal pressure level is a symptom of not just glaucoma. For example, Meniere’s disease is associated with chronically high endolymphatic pressure, which distends fluid compartments of the cochlea and compresses the neurosensory organ[18,28,32]. As with

glaucoma, animal models of Meniere's disease attempt to induce cochlear hypertension via surgical, mechanical, or pharmacological methods oftentimes with inconsistent and irreversible results. The iPump system could thus provide a useful tool for investigating the etiology and pathophysiology of a myriad of pressure-induced neurodegenerative diseases.

Comparisons to existing technologies

Several noninvasive and invasive technologies are commercially available for IOP measurement. Noninvasive technologies like the gold-standard applanation tonometer and cutting-edge wireless contact lens sensors[13,17] are appealing because data can be obtained quickly with minimal subject preparation or trauma. However, the IOP readings are indirect and thus not absolute[1]. With tonometers they are also sparse and sporadic since readings are made by hand. Invasive technologies exist that can be placed inside the eye[11,33,35] or connected to the eye via a tube[2,8,15,19]. They require surgical training and open the eye to surgical complications but also give round-the-clock streams of IOP data with little need for experimenter involvement. The iPump system measures IOP with open-loop accuracy of 0.2 mmHg and closed-loop accuracy of 0.7 mmHg, which meets or exceeds commercial systems (Konigsberg and DSI) that have been used for chronic IOP recording[2,8,15,19]. The iPump is not yet implantable like those systems, but it is only available technology that can automatically regulate IOP.

Current limitations of the technology

The iPump system is intended for use on conscious animals, which presents design issues for consideration. One is reservoir size. The aqueous humor volume and outflow facility of rat eyes is ~10 μl^3 and ~0.05 μl/min/mmHg[12,21], respectively, meaning that a sustained IOP increase of 10 mmHg translates to an outflow of ~0.7 ml/day or ~7 eye volumes/day. The reservoir will thus need weekly refilling and perhaps resizing for other research applications or animals. Another is system tethering. Since the iPump sensor is outside the eye, vertical animal movement can cause hydrostatic pressure differences between the eye and sensor and introduce motion artifacts into the IOP record. Rats are small and live mostly in one horizontal plane, so the artifacts would be a few mmHg at most and minimally affect iPump operation. They would get filtered by control circuitry and the programmable window about which the system holds IOP. The tethered version described here would not be suitable for large upright animals, such as monkeys. An implantable version of the iPump would be required.

ACKNOWLEDMENTS

The work was supported by NIH grant R21 EY023376 and a Thomas R. Lee Award from the BrightFocus Foundation. The authors thank Drs. Radouil Tzekov and Xiaolan Tang for assistance with histological processing, Dr. Wilfredo Moreno for consultations with controller design, and Dr. Curtis Margo for evaluating the pathology of implanted eyes. The authors declare the following intellectual interests: U.S. patents 9,022,968 B2 and 9,314,375 B1.

REFERENCES

1. Abrams LS, Vitale S, Jampel HD. Comparison of three tonometers for measuring intraocular pressure in rabbits. Invest. Ophthalmol. Vis. Sci. 1996; 37:940–944. [PubMed: 8603880]

2. Akaishi T, Ishida N, Shimazaki A, Hara H, Kuwayama Y. Continuous monitoring of circadian variations in intraocular pressure by telemetry system throughout a 12-week treatment with timolol maleate in rabbits. J. Ocul. Pharmacol. Therap. 2005; 21:436–444. [PubMed: 16386085]

3. Akula JD, Favazza TL, Mocko JA, Benador IY, Asturias AL, Kleinman MS, Hansen RM, Fulton AB. The anatomy of the rat eye with oxygen-induced retinopathy. Doc. Ophthalmol. 2010; 120:41–50. [PubMed: 19820974]

4. Asrani S, Zeimer R, Wilensky J, Gieser D, Vitale S, Lindenmuth K. Large diurnal fluctuations in intraocular pressure are an independent risk factor in patients with glaucoma. J. Glaucoma. 2000; 9:134–142. [PubMed: 10782622]

5. Bengtsson B, Leske MC, Hyman L, Heijl A. Fluctuation of intraocular pressure and glaucoma progression in the early manifest glaucoma trial. Ophthalmol. 2007; 114:205–209.

6. Berdahl JP, Fautsch MP, Stinnett SS, Allingham RR. Intracranial pressure in primary open angle glaucoma, normal tension glaucoma, and ocular hypertension: a case– control study. Invest. Ophthalmol. Vis. Sci. 2008; 49:5412–5418. [PubMed: 18719086]

7. Chauhan BC, Pan J, Archibald ML, LeVatte TL, Kelly ME, Tremblay F. Effect of intraocular pressure on optic disc topography, electroretinography, and axonal loss in a chronic pressure-induced rat model of optic nerve damage. Invest Ophthalmol Vis Sci. 2002; 43:2969–2976. [PubMed: 12202517]

8. Downs JC, Burgoyne CF, Seigfreid WP, Reynaud JF, Strouthidis NG, Sallee V. 24-hour IOP telemetry in the nonhuman primate: implant system performance and initial characterization of IOP at multiple timescales. Invest. Ophthalmol. Vis. Sci. 2011; 52:7365–7375. [PubMed: 21791586]

9. Fitt AD, Gonzalez G. Fluid mechanics of the human eye: aqueous humour flow in the anterior chamber. Bull. Mathemat. Bio. 2006; 68.1:53–71.

10. Gaasterland D, Kupfer C. Experimental glaucoma in the rhesus monkey. Invest. Ophthalmol. Vis. Sci. 1974; 13:455–457.

11. Ha D, de Vries WN, John SW, Irazoqui PP, Chappell WJ. Polymer-based miniature flexible capacitive pressure sensor for intraocular pressure (IOP) monitoring inside a mouse eye. Biomed. Microdevices. 2012; 14:207–15. [PubMed: 21987004]

12. Kee C, Hong T, Choi K. A sensitive ocular perfusion apparatus measuring outflow facility. Curr. Eye Res. 1997; 16:1198–201. [PubMed: 9426951]

13. Leonardi M, Pitchon EM, Bertsch A, Renaud P, Mermoud A. Wireless contact lens sensor for intraocular pressure monitoring: assessment on enucleated pig eyes. Acta Ophthalmol. 2009; 87:433–437. [PubMed: 19016660]

14. Leske MC, Connell AM, Wu SY, Hyman LG, Schachat AP. Risk factors for open-angle glaucoma: the Barbados Eye Study. Arch. Ophthalmol. 1995; 113:918–924. [PubMed: 7605285]

15. Li R, Liu JH. Telemetric monitoring of 24 h intraocular pressure in conscious and freely moving C57BL/6J and CBA/CaJ mice. Mol. Vision. 2008; 14:745–749.

16. Liu JH, Zhang X, Kripke DF, Weinreb RN. Twenty-four-hour intraocular pressure pattern associated with early glaucomatous changes. Invest. Ophthalmol. Vis. Sci. 2003; 44:1586–1590. [PubMed: 12657596]

17. Mansouri K, Medeiros FA, Tafreshi A, Weinreb RN. Continuous 24-hour monitoring of intraocular pressure patterns with a contact lens sensor: safety, tolerability, and reproducibility in patients with glaucoma. Arch. Ophthalmol. 2012; 130:1534–1539.

18. Mateijsen DJ, Rosingh HJ, Wit HP, Albers FW. Perilymphatic pressure measurement in patients with Meniere's disease. Euro. Arch. Otorhinolaryngol. 2001; 258:1–4.

19. McLaren JW, Brubaker RF, Fitzsimon JS. Continuous measurement of intraocular pressure in rabbits by telemetry. Invest. Ophthalmol. Vis. Sci. 1996; 37:966–975. [PubMed: 8631640]

20. McNulty R, Wang H, Mathias RT, Ortwerth BJ, Truscott RJ, Bassnett S. Regulation of tissue oxygen levels in the mammalian lens. J. Physiol. 2004; 559:883–898. [PubMed: 15272034]

21. Mermoud A, Baerveldt G, Minckler DS, Prata JA Jr, Rao NA. Aqueous humor dynamics in rats. Graefes Arch. Clin. Exp. Ophthalmol. 1996; 234:S198–203. [PubMed: 8871174]

22. Moore CG, Johnson EC, Morrison JC. Circadian rhythm of intraocular pressure in the rat. Curr. Eye Res. 1996; 15:185–191. [PubMed: 8670727]

23. Morrison JC, Moore CG, Deppmeier LM, Gold BG, Meshul CK, Johnson EC. A rat model of chronic pressure-induced optic nerve damage. Exp. Eye Res. 1997; 64:85–96. [PubMed: 9093024]
24. Nusbaum DM, Wu SM, Frankfort BJ. Elevated intracranial pressure causes optic nerve and retinal ganglion cell degeneration in mice. Exp. Eye Res. 2015; 136:38–44. [PubMed: 25912998]
25. Quigley HA, Addicks EM. Chronic experimental glaucoma in primates. I. Production of elevated intraocular pressure by anterior chamber injection of autologous ghost red blood cells. Invest. Ophthalmol. Vis. Sci. 1980; 19:126–136. [PubMed: 6766124]
26. Ren R, Jonas JB, Tian G, Zhen Y, Ma K, Li S, Wang H, Li B, Zhang X, Wang N. Cerebrospinal fluid pressure in glaucoma: a prospective study. Ophthalmology. 2010; 117:259–66. [PubMed: 19969367]
27. Ruiz-Ederra J, García M, Hernández M, Urcola H, Hernández-Barbáchano E, Araiz J, Vecino E. The pig eye as a novel model of glaucoma. Exp. Eye Res. 2005; 81:561–569. [PubMed: 15949799]
28. Salt AN, Plontke AK. Endolymphatic hydrops pathophysiology and experimental models. Otolaryngol. Clin. North Am. 2010; 43:971–983. [PubMed: 20713237]
29. Sappington RM, Carlson BJ, Crish SD, Calkins DJ. The microbead occlusion model: a paradigm for induced ocular hypertension in rats and mice. Invest. Ophthalmol.Vis. Sci. 2010; 51:207–216. [PubMed: 19850836]
30. Shareef SR, Garcia-Valenzuela E, Salierno A, Walsh J, Sharma SC. Chronic ocular hypertension following episcleral venous occlusion in rats. Exp. Eye Res. 1995; 61:379–382. [PubMed: 7556500]
31. Sommer A. Intraocular pressure and glaucoma. Am. J. Ophthalmol. 1989; 107:186–188. [PubMed: 2913813]
32. Takumida M, Akagi N, Anniko M. A new animal model for Meniere's disease. Acta Otolaryngol. 2008; 128:263–71. [PubMed: 17851960]
33. Todani A, Behlau I, Fava MA, Cade F, Cherfan DG, Zakka FR, Jakobiec FA, Gao Y, Dohlman CH, Melki SA. Intraocular pressure measurement by radio wave telemetry. Invest. Ophthalmol. Vis. Sci. 2011; 52:9573–9580. [PubMed: 22039243]
34. Ueda J, Sawaguchi S, Hanyu T, Yaoeda K, Fukuchi T, Abe H, Ozawa H. Experimental glaucoma model in the rat induced by laser trabecular photocoagulation after an intracameral injection of India ink. Jap. J. Ophthalmol. 1998; 42:337–344. [PubMed: 9822959]
35. Walter P, Schnakenberg U, vom Bögel G, Ruokonen P, Krüger C, Dinslage S, Lüdtke Handjery HC, Richter H, Mokwa W, Diestelhorst M, Krieglstein GK. Development of a completely encapsulated intraocular pressure sensor. Ophthalmic Res. 2000; 32:278–284. [PubMed: 11015039]
36. Weber AJ, Zelenak D. Experimental glaucoma in the primate induced by latex microspheres. J. Neurosci. Meth. 2001; 111:39–48.

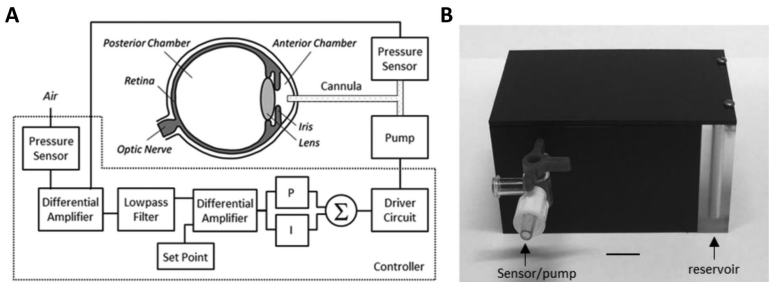

Figure 1.

IOP control system. (A) Block diagram of the system. A pressure sensor measures IOP via a fine cannula implanted in the anterior chamber of the eye and a second sensor measures atmospheric pressure. A controller circuit amplifies and filters the difference in pressure signals and compares the result against a user-specified set point. If IOP deviates from the desired level, proportional (P) and integrator (I) circuit elements combine to produce a command signal that drives a small pump to inject or withdraw fluid through the cannula until IOP returns to the set point. (B) Picture of portable iPump system. All electronic components are housed in a small plastic box (8 × 5 × 4 cm) that contains a fluid reservoir which can be filled or drained. The box tethers to the animal via tubing that runs inside a protective spring to a plastic head mount which connects subdermally to the implanted cannula. Bar: 1 cm.

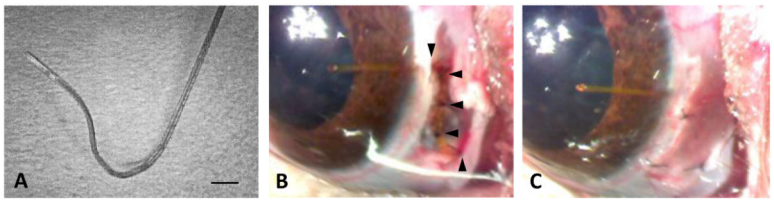

Figure 2.

Eye implantation procedure. (A) Cannula pre-shaped for rat eyes with heat. Bar: 500 μm. (B) Cannula implanted in the anterior chamber of a rat eye and secured with half-thickness sutures (arrowheads) to the sclera. (C) Rat eye after cannula implantation

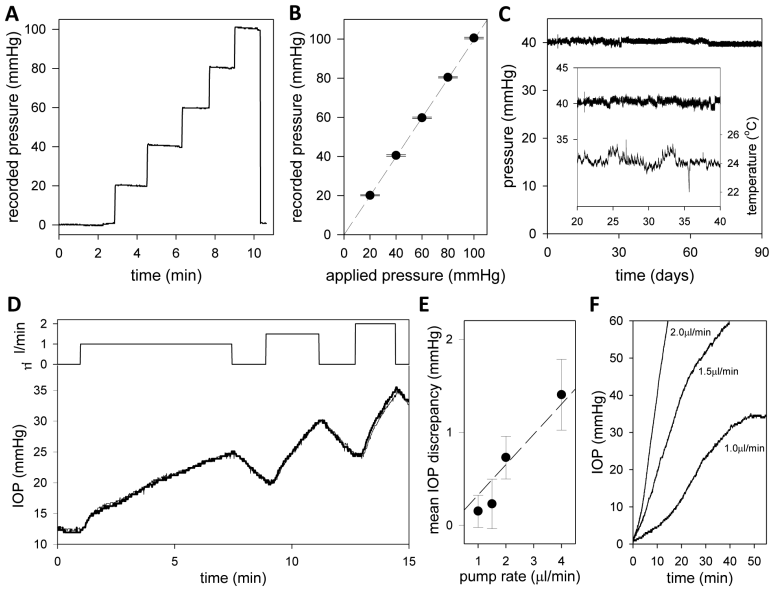

Figure 3.

iPump system properties. (A) System output as applied pressure was raised in steps of 20 mmHg every 1-2 minutes and released. (B) Mean (symbols) and standard deviation (bars) of pressure readings for each step in applied pressure. (C) Signal recorded over 90 days with applied pressure set at 40 mmHg. Data were fit by the regression line: $f(x) = 40.7 - 0.0077x$. Inset, segment of the pressure record during which room temperature fluctuated greatest. (D) Top: Time course of pump rates applied by the system to a dead rat eye in situ. The rate was stepped on and off to 1, 1.5 and 2uL/min over a 15-min period. Bottom: Pump-induced IOP changes recorded simultaneously by the iPump (thick line) and a second pressure sensor (thin line) independently connected to the eye. (E) Mean and standard deviation of the difference record obtained by subtracting the simultaneously-recorded IOP signals for pump rates of 1 to 4uL/min. Dashed line estimates the system resistance based on Pouiselle's law . (F) IOP dynamics following the perfusion rate steps.

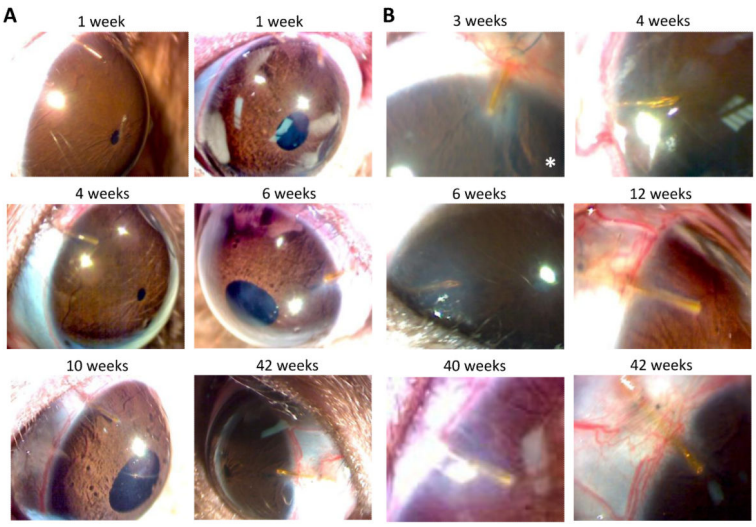

Figure 4.

Rat eyes with chronically implanted cannulas. (A) Time series of images of two rat eyes implanted with a cannula for over 3 months (I4: left) and 10 months (I10: right). (B) Magnified images of the cannula tip in these (I4: right middle, I10: right bottom) and four other animals at experiment end. Asterisk indicates an eye that exhibited a local corneal response to the implant.

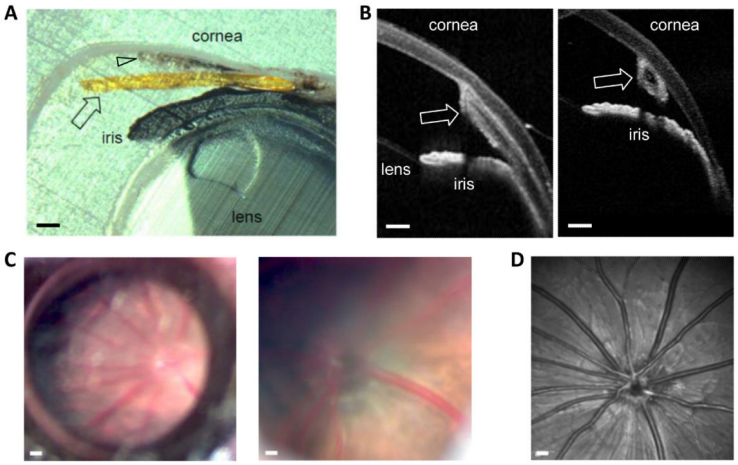

Figure 5.

Internal structure of an implanted rat eye (I4). (A) Iridocorneal angle after fixation and paraffin embedding. Arrows mark the cannula. Arrowhead points to scar tissue growth between the cornea and cannula. Bars: 200μm. (B) Iridocorneal angle viewed along the longitudinal (left) and transverse (right) plane of the cannula. Images were acquired at experiment end with a Heidelberg-Spectralis II OCT scanner with the rat under anesthesia. (C) Fundus viewed at low (left) and high (right) magnification via a digital stereoscope, ring light, and coverslip on the cornea. Bars: 500μm and 200μm. (D) Fundus image acquired at experiment end with the OCT scanner. Bar: 500μm.

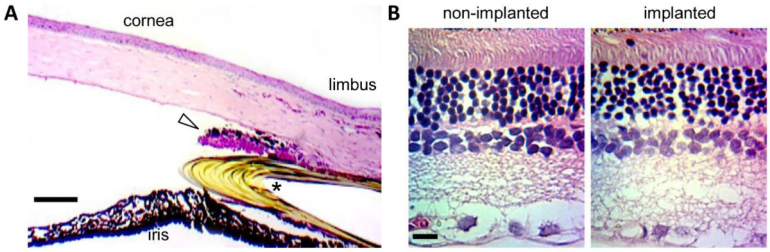

Figure 6.

Histology of an implanted rat eye (I4). (A) HE stained section of the iridocorneal angle. Asterisk marks the cannula. Triangle points at an outgrowth of scar tissue. Bar: 100μm. (B) HE stained section of the retina of the non-implanted and implanted eyes. Inspection of serial retinal sections all presented similar cell density and layer thickness. Bar: 25μm.

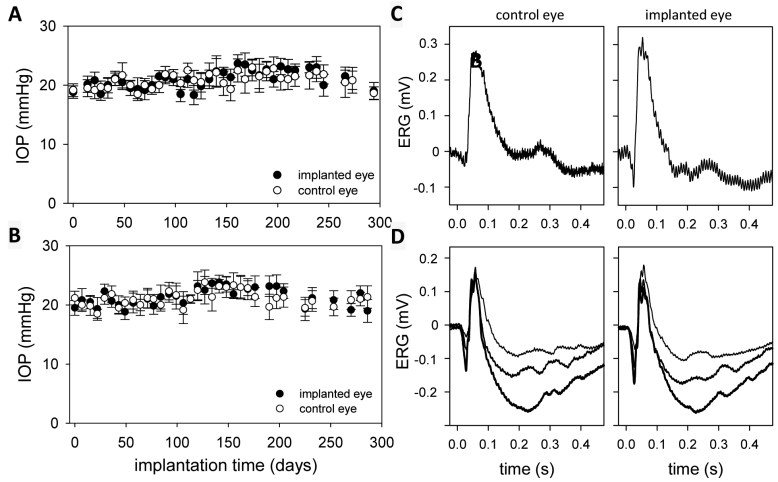

Figure 7.

(A,B) IOP history of implanted rat eyes (A: I10, B: I14). Each data point is the average of 6 tonometer readings. Bars are standard deviation. (C,D) Flash ERG records of implanted and non-implanted eyes of two rats (C: I4, D: I10) after 6 weeks. Each record is the average of 30 responses to full-field flashes with an interstimulus interval of 3 s. Flash intensity: 4.3 (thin trace), 8.6 (thicker trace), and 17.2 kcd/m^2 (thickest trace).

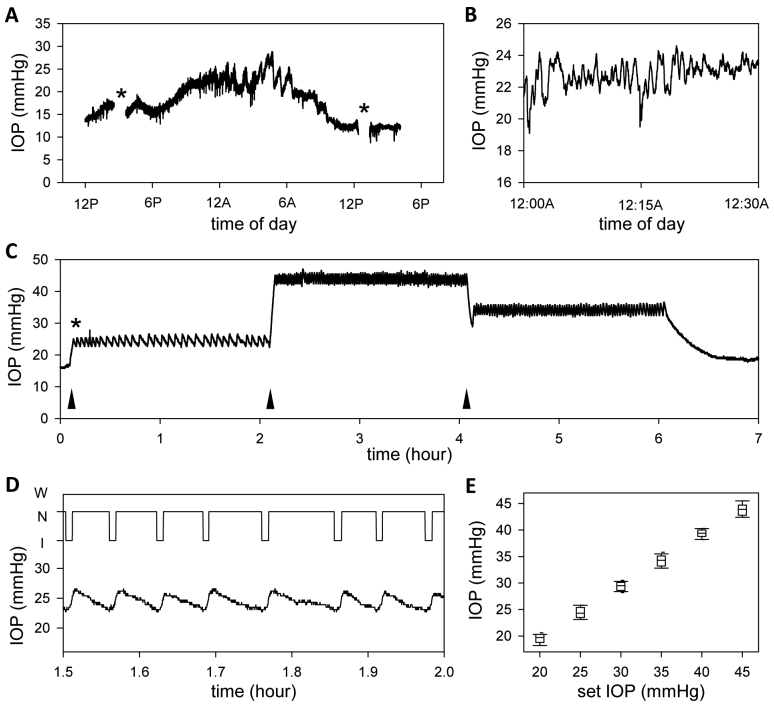

Figure 8.

IOP monitoring and controlling with the iPump system. (A) IOP record of the implanted eye of an anesthetized rat. Asterisks mark data periods that were excluded because IOP was manipulated to examine system behavior. (B) Short (30-min) segment of the IOP record at midnight. (C) IOP record of the implanted eye of an anesthetized rat during which the system was programmed to hold pressure at 25, 45, and 35 mmHg for 2 hours each. Asterisk marks the start of IOP control. Arrowheads mark the start of each IOP step. (D) Top, record of pump action (I: injection, N: neutral, W: withdrawal) for a 30-min period. Bottom, IOP dynamics over the same period. (E) Box-and-whiskers plot of the distribution of IOP readings for each IOP step. Center line: mean IOP, lower and upper edges: 25% to 75% range, lower and upper whiskers: 10^{th} and 90^{th} data percentiles.